

Magneto-Ferroelectric Interaction in Superlattices: Monte Carlo Study of Phase Transitions

I. F. Sharafullin ^{a,b}, M. Kh. Kharrasov ^b, H. T. Diep* ^a

^a *Laboratoire de Physique Théorique et Modélisation,*

Université de Cergy-Pontoise, CNRS, UMR 8089,

2 Avenue Adolphe Chauvin, 95302 Cergy-Pontoise, Cedex, France.

^b *Bashkir State University, 32, Validy str, 450076, Ufa, Russia.*

We study in this paper the phase transition in superlattices formed by alternate magnetic and ferroelectric layers, by the use of Monte Carlo simulation. We study effects of temperature, external magnetic and electric fields, magnetoelectric coupling at the interface on the phase transition. Magnetic layers in this work are modeled as thin films of simple cubic lattice with Heisenberg spins. Electrical polarizations of ± 1 are assigned at simple cubic lattice sites in the ferroelectric layers. The transition temperature, the layer magnetizations, the layer polarizations, the susceptibility, the internal energy, the interface magnetization and polarization are calculated. The layer magnetizations and polarizations as functions of temperature are shown for various coupling interactions and field values. Mean-field theory is also presented and compared to MC results.

PACS numbers: 05.10.Ln, 05.10.Cc, 62.20.-x

Keywords: phase transitions, superlattice, Monte Carlo simulation, magnetoelectric interaction

I. INTRODUCTION.

The study of phase transitions, surface effects and critical phenomena in superlattices or multilayered magnetic nanofilms has been rapidly developed during the last two decades (see reviews¹⁻⁵). Such high interest in this area was stimulated by the fact that superlattices of nanofilm and multiferroics possess a number of unique properties which have a

* Corresponding author, diep@u-cergy.fr

broad area of applications in nanoelectronics, spintronics^{2,6-11} and devices using the giant magnetoresistance phenomenon^{1,3,12}.

With modern technologies it is possible to create superlattices and multilayer nanofilms as thin as a few atomic layers from the crystal structures with magnetic and ferroelectric orderings. These structures are able to manifest magnetoelectric effects which are known to be the result of interactions between magnetic and ferroelectric subsystems. It should be noted that the study of magnetoelectric effects in these systems draws a great fundamental interest for their special features, such as size dependence of magnetic and ferroelectric order parameters and other characteristics^{6,7,13,14}. For example, it has been shown that the change from the bulk values for films of a few dozens of monolayers ($d \geq 10$ nm) to the two-dimensional values for films thinner than 4-6 monolayers ($d \leq (1 - 2)$ nm)^{3,13}.

In Ref. 15 it was shown that in heterostructures with magnetic and ferroelectric materials, the magnetoelectric effect induced by an external electric field is observed at the interface layer. This effect is accompanied by the appearance of an antiferromagnetic phase at the interface as well as with the change in the critical temperature of the magnetic layer. This has been observed experimentally in $\text{La}_{0.87}\text{Sr}_{0.13}\text{MnO}_3 / \text{PbZr}_{0.52}\text{Ti}_{0.48}\text{O}_3$ ¹⁶ at certain concentrations of manganite. In the work Ref. 17 with Monte Carlo (MC) simulation for a two-layer film with the structure $\text{LaSrMnO} / \text{PbZrTiO}$, phase transitions have been investigated and the correctly describing model has been proposed. A multi-sublattice model has been introduced to explain magnetic properties of compounds R_2Fe_{17} , $\text{Ho}_2\text{Fe}_{11}\text{Ti}$ and TbMn_6Sn_6 ¹⁸⁻²⁰.

On theoretical points of view, one of the most studied systems for the layered magnetic structure was concentrated on the magnetic properties of magnetic bilayer²¹. Wei Wang et al.²² have studied a ferrimagnetic mixed spin (1/2, 1) Ising double layer superlattice: they have shown the effects of the exchange coupling and the layer thickness on the compensation behavior and magnetic properties of the system, by MC simulation. Some interesting phenomena have been found, such as various types of magnetization curves, originating from the competition between the exchange coupling and temperature. In Ref. 23 the phase diagram and magnetic properties of the mixed spin (1, 3/2) Ising ferroelectric superlattices with alternate layers have been investigated by means of MC simulation. It should be noted that they also investigated superlattice of only two ferroelectric layers with antiferroelectric interfacial interaction between layers, within the transverse Ising model. They found a

number of interesting phenomena, such as the existence of the compensation temperature or transverse field to compensate the specific ranges of exchange interactions.

Note that MC methods based on the Metropolis algorithm, as well as other algorithms have proven to be successful in describing physical properties of magnetic systems of different spatial dimensions. They revealed particular features of the phase transitions in these systems²⁴. In Refs. 3, 25, 26 and 27 numerical studies of size effects in critical properties of the Heisenberg multilayer films with MC methods were conducted. For films of varying thickness an anisotropy induced, for example, by the crystalline field of the substrate, was taken into account. The precise calculation of critical indices was carried, the values of which have clearly demonstrated the dimensional transition from two-dimensional to three-dimensional properties of the films with increasing number of layers.

In this paper the methodology for Heisenberg multilayer films simulations^{1,24} is used for the MC simulation and the calculation of magnetic properties of multiferroic superlattices. Although previous valuable theoretical, numerical and experimental studies have been done, more research is still needed to further understand the magnetic, ferroelectric and thermodynamic properties of the superlattice. Our investigation is motivated by the fact that superlattices with magnetic and ferroelectric materials present great opportunities of applications in spintronics.

In the present paper, we will thus study the effects of the magnetoelectric coupling and the external magnetic and electric fields on the magnetic properties of the multiferroic superlattice shown in Fig. 1.

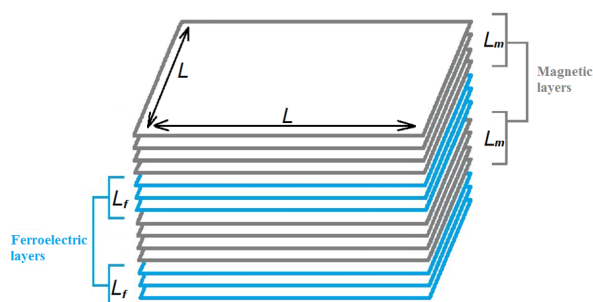


FIG. 1: Schematic representation of the superlattice: alternate ferroelectric and magnetic films.

The paper is organized as follows. The model of the superlattice is presented in section II, where we summarize the principal steps used in the calculation of the ground-state configurations of the system. Section III shows the MC results of energy, layer magnetizations, susceptibilities and layer polarizations. Section IV shows results of another choice for interface coupling. The mean-field (MF) theory is shown in section V. Concluding remarks are given in section VI.

II. MODEL AND GROUND STATE

A. Model

We consider a multilayer multiferroic films composed of L_z^m ferromagnetic layers and L_z^f ferroelectric layers alternately sandwiched in the z direction (see Fig. 1). Each xy plane has the dimension $L \times L$. The lattice sites of the magnetic layers of this superlattice are occupied by interacting Heisenberg spins \vec{S}_i , while the lattice sites of the ferroelectric layers are occupied by interacting polarizations $\vec{P} = \pm 1$ along the z axis. Our system thus consists of a $L \times L \times L_z$ sites where $L_z = L_z^m + L_z^f$. We assume periodic boundary conditions in all directions to reduce surface effects. We assume interactions between ferroelectric and magnetic systems at their interfaces. The Hamiltonian of the system is defined as follows:

$$\mathcal{H} = H_m + H_f + H_{mf}, \quad (1)$$

The first term is the Hamiltonian of the magnetic subsystem, the second - of the ferroelectric subsystem, the third term is the Hamiltonian of their interaction. We assume

$$H_m = - \sum_{i,j} J_{ij}^m \vec{S}_i \cdot \vec{S}_j - \sum_i (\vec{H} \cdot \vec{S}_i) \quad (2)$$

here $J_{ij}^m > 0$ characterizes the ferromagnetic interaction between one spin and its nearest neighbors (NN). We consider it to be the same for NN within a layer and NN in adjacent layers. \vec{S}_i is the classical Heisenberg spin occupying the i -th site. \vec{H} is an applied magnetic field along the $+z$ direction. For the ferroelectric subsystem we write

$$H_f = - \sum_{i,j} J_{ij}^f P_i P_j - \sum_i P_i E^z \quad (3)$$

where P_i is the polarization along the z axis at the i -th site assumed to have only two values ± 1 (Ising-like model), $J_{ij}^f > 0$ denotes the NN ferroelectric interaction, similar for all NN. $E^z > 0$ is the external electric field applied along the $+z$ axis perpendicular to the plane of the layers.

The magnetic interface layer creates at a site k of the ferroelectric interface an effective field $H(k)$ along z axis which is

$$H(k) = -J_{mf1} \sum_{i,j} \vec{S}_i \cdot \vec{S}_j - J_{mf2} \sum_{i,j} \vec{S}_i \cdot \vec{S}_j, \quad (4)$$

so that the energy of interface magnetoelectric interaction of the polarization at the site k can be written as

$$H_{mf}(k) = H(k) P_k, \quad (5)$$

In this expression J_{mf1} is the interaction parameter between the electric polarization component P_k at the interface ferroelectric layer and its NN spin on the adjacent magnetic layer. J_{mf2} is the interaction parameter between the electric polarization component P_k at the interface ferroelectric layer and the next NN spin on the adjacent magnetic layer. These interactions are shown schematically in the Fig. 4.

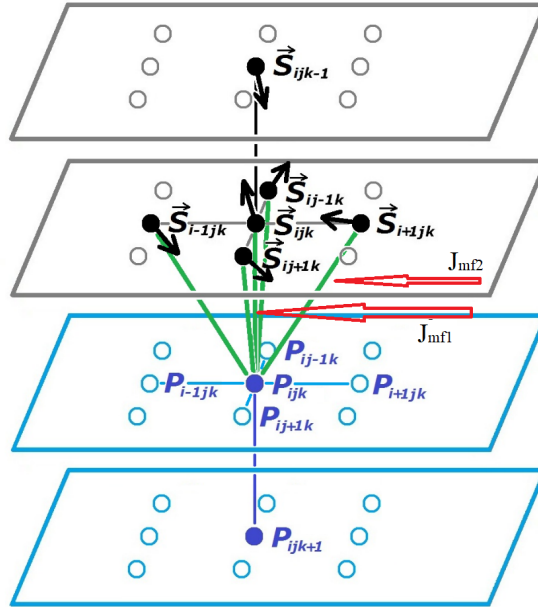


FIG. 2: Schematic representation of magnetoelectric interactions at the interface between magnetic and ferroelectric layers.

Note that the interface coupling described by Eq. (5) is a scalar spin field acting on an electric polarization. Later, in section IV we will suppose another form for the coupling: a scalar polarization field acting on the z spin component.

B. Ground state

Let us take positive J_{ij}^m and J_{ij}^f so that magnetic layers are ferromagnetic and ferroelectric layers have parallel polarizations, in the ground state.

The relative orientation between two adjacent magnetic and ferroelectric layers depends on the signs of J_{mf1} and J_{mf2} . There are two simple cases:

i) if they are both positive, then spins and polarizations are parallel in the ground state (GS)

ii) if they are negative, then spins are antiparallel to polarizations in the GS.

The complicated case occurs when J_{mf1} and J_{mf2} have opposite signs. In this case, there is a competition between them which gives rise to some degree of frustration. For example, when $J_{mf1} > 0$ and $J_{mf2} < 0$ we have the situation where NN interaction wants \vec{S} and \vec{P} to be parallel, while the NNN interaction wants them to be antiparallel. Depending on their respective amplitudes, one configuration wins over the others.

Let us write the GS energy of a spin at the interface in zero fields

$$E_1 = -Z_1 J^m - Z_2 J_{mf1} - Z_3 J_{mf2} \quad (6)$$

where the coordination numbers are $Z_1 = 4, Z_2 = 1, Z_3 = 4$ for a simple cubic lattice.

For $J_{mf1} < 0$, the four spin configurations (see Fig. 3)

$$E_1 = -Z_1 J^m - Z_2 |J_{mf1}| - Z_3 |J_{mf2}| \quad (7)$$

$$E_2 = -Z_1 J^m + Z_2 |J_{mf1}| - Z_3 J_{mf2} \quad (8)$$

$$E_3 = -Z_1 J^m - Z_2 |J_{mf1}| + Z_3 J_{mf2} \quad (9)$$

$$E_4 = +Z_1 J^m - Z_2 |J_{mf1}| - Z_3 J_{mf2} \quad (10)$$

where E_1 is the energy of the state where all spins are down, all polarizations are up with $J_{mf2} < 0$ (Fig. 3a). Other energies correspond to the spin configurations shown in Fig. 3: E_2 to Fig. 3b with $J_{mf2} > 0$, E_3 to Fig. 3c with $J_{mf2} > 0$ and E_4 to Fig. 3d with $J_{mf2} > 0$.

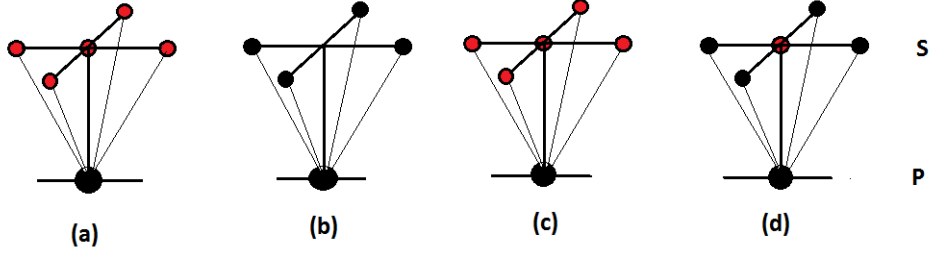


FIG. 3: Ground state spin configurations with energies from E_1 to E_4 (a to d, respectively) depending on the interface interactions between magnetic and ferroelectric layers. Lower black circles are $P = 1$ (up), upper black circles are up spins, red circles are down spins.

The system will choose the GS depending on the values of J_{mf1} and J_{mf2} . For simplicity, let us confine ourselves to GS configurations where all magnetic spins are parallel and all polarizations are parallel, i. e. the first three configurations. This choice is possible if the intralayer interactions $J^m > 0$ and $J^f > 0$ are sufficiently strong.

The state E_1 is chosen if

$$E_1 < E_2, E_1 < E_3, E_1 < E_4 \quad (11)$$

Solving these inequalities we have

$$J_{mf2} < 0, |J_{mf1}| < \frac{Z_1 J^m - Z_3 J_{mf2}}{Z_2}, |J_{mf1}| > 0 \quad (12)$$

namely,

$$J_{mf2} < 0, |J_{mf1}| < 4(J^m - J_{mf2}), J_{mf1} < 0 \quad (13)$$

Now we suppose $J_{mf2} > 0$ then the GS will change to E_2 . The critical value of J_{mf2} and J_{mf1} are determined by solving

$$E_2 < E_1, E_2 < E_3, E_2 < E_4 \quad (14)$$

We have

$$J_{mf2} > 0, J_{mf1} < \frac{Z_3 J_{mf2}}{Z_2}, |J_{mf1}| < \frac{Z_1 J^m}{Z_2} \quad (15)$$

namely,

$$J_{mf2} > 1/4|J_{mf1}|, J_{mf2} > 0, |J_{mf1}| < 4J_m \quad (16)$$

The GS is E_3 if we have

$$E_3 < E_1, E_3 < E_4, E_3 < E_2 \quad (17)$$

We get

$$|J_{mf1}| > 0, J_{mf2} < \frac{Z_2|J_{mf1}|}{Z_3}, J_{mf2} < \frac{Z_1J^m}{Z_3} \quad (18)$$

or

$$J_{mf2} < 1/4|J_{mf1}|, J_{mf2} < J^m, |J_{mf1}| > 0 \quad (19)$$

In MC simulations shown below, care should be taken to choose the right GS according to values and signs of the interface interactions to avoid metastable states at low temperatures (T).

Note that we have taken $J_{mf1} < 0$ in the above spin configurations. This is intended to have spins antiparallel to the magnetic field applied in the $+z$ direction so as to have a phase transition at a temperature with a finite field.

III. MONTE CARLO SIMULATION

For MC simulations we use the Metropolis algorithm and a sample size $L \times L \times L_z$ with $L = 40, 60, 80, 100$ for detection of lateral size effects and $L_z = 8, 16, 12, 24$ for thickness effects. When we investigate the effects of the magnetoelectric coupling on the magnetic, ferroelectric and interface properties, for simplicity we take the same size and thickness for the ferroelectric and magnetic layers (for example if $L_z = 8$ - it means $L_z^m = 4$ magnetic layers and $L_z^f = 4$ ferroelectric layers). Exchange parameters between intralayer spins and intralayer polarizations are taken to be $J^m = J^f = 1$ for the simulation.

For MC simulation we perform the cooling from the disordered phase: electrical polarizations of ± 1 are randomly assigned at lattice sites in the ferroelectric layers, in the z direction. In the ferromagnetic layers spins with $|\vec{S}| = 1$ are also randomly assigned in any direction, following in the spatial uniform distribution. At each T , new random \vec{S}_i and P_i were chosen, and the energy difference caused by this change is calculated. This change is accepted or rejected according to the Metropolis algorithm. In order to ensure the convergence of the observables, the lattice is swept 100000 times, where each time is considered as one MC step

(MCS) that can be taken as the time scale of simulations. The observables of interest such as the averages of layer electric polarizations P , and layer magnetization M , are calculated over the following 50000 MCS. These quantities are defined as

$$P(n) = \frac{1}{L^2} \langle |\sum_{i \in n} P_i| \rangle \quad (20)$$

$$M(m) = \frac{1}{L^2} \langle |\sum_{j \in m} \vec{S}_j| \rangle \quad (21)$$

where $\langle \dots \rangle$ is the time average, and the sums on i and j are performed over the lattice sites belonging to the ferroelectric layer n and the lattice sites belonging to the magnetic layer m , respectively. The process is repeated for a lower T down to the desirable lowest one. We also perform the heating, starting from the GS spin configuration.

A. Zero fields

Monte Carlo results for energy, magnetization and polarization and their susceptibilities obtained by heating the system from the initial spin configuration of GS energy E_1 are shown in Fig. 4. Of course, starting from different initial spin configurations which are not the GS will lead to the same thermodynamic equilibrium but the equilibrating time is longer in particular at low T .

MC results for energy, magnetization and polarization and their susceptibilities obtained by heating the initial spin configurations of energy E_2 are shown in Fig. 5. For E_3 , the results are qualitatively similar (not shown). respectively.

The above figures show that the energy and other physical quantities well behave at low T (no metastability) if we choose the correct GS according to the interface interaction. Note that the ferroelectric films undergo a phase transition at a temperature higher than that of the magnetic films. This is due to the Ising-like nature of the ferroelectric polarizations (in the bulk, the transition temperature is inversely proportional to N , the spin components, $\sim 1/N$). Also, the interface layers have lightly smaller order parameter than those inside the films.

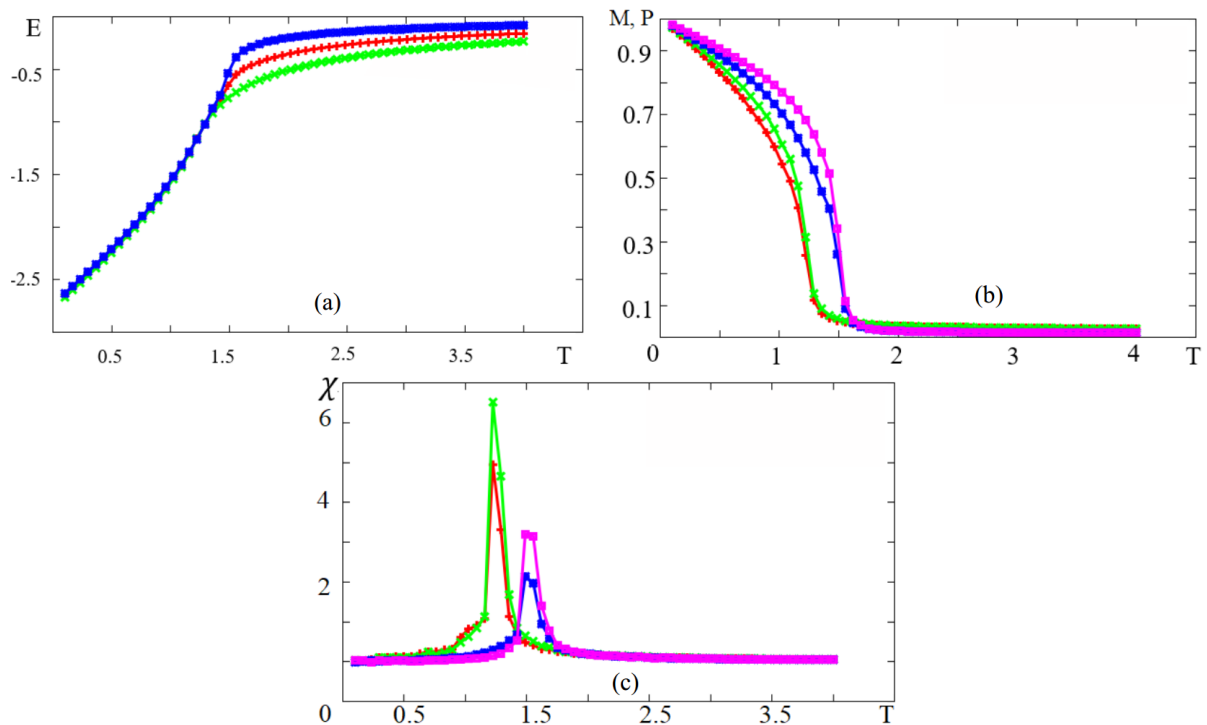


FIG. 4: (a) Energy versus T . Red line: energy for total superlattice, green line: energy of magnetic layers, blue line: energy of ferroelectric layers ; (b) Magnetization and polarization versus T . Red line: magnetization of interface magnetic layers, green line: magnetization of interior magnetic layers, blue line: polarization of interface ferroelectric layers, purple line: polarization of interface ferroelectric layers ; (c) Susceptibilities versus T , with the same color code. $J^m = 1, J_{mf1} = -0.15, J_{mf2} = -0.135$ corresponding to the GS with energy E_1 .

B. Particular Case $J_{mf1} = J_{mf2}$

In this section we present the results of the MC simulations in the particular case where $J_{mf1} = J_{mf2}$. We will compare these results with results from the MF theory.

Results for the temperature dependence of layer magnetizations, polarizations, and susceptibilities of the system are shown in Fig. 6 for $J_m = J_f = 1, J_{mf} = J_{mf1} = J_{mf2} = -0.15, -0.55$. For J_{mf} , these curves present a sharp second-order transitions at $T_c^m \simeq 1.32$ for magnetic layers and $T_c^f \simeq 1.84$ for ferroelectric layers.

The results with an external magnetic field $H^z = 0.7$ are shown in Fig. 7 for the order

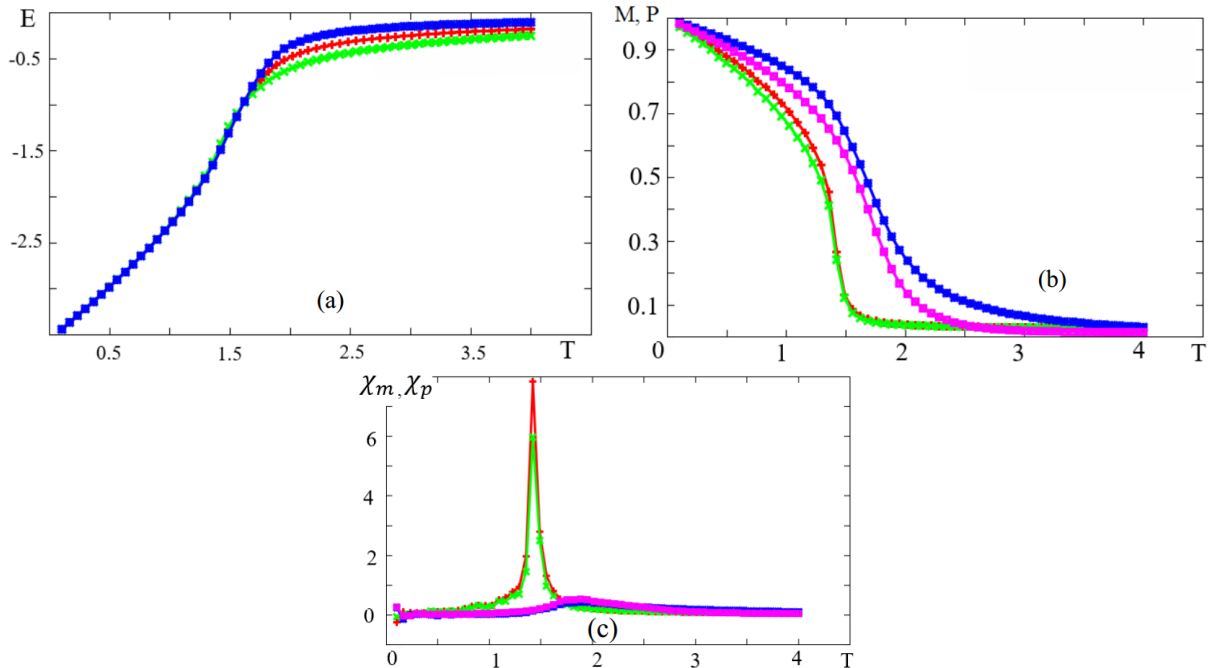


FIG. 5: (a) Energy versus T . Red line: energy for total superlattice, green line: energy of magnetic layers, blue line: energy of ferroelectric layers ; (b) Magnetization and polarization versus T . Red line: magnetization of interface magnetic layers, green line: magnetization of interior magnetic layers, blue line: polarization of interface ferroelectric layers, purple line: polarization of interface ferroelectric layers ; (c) Susceptibilities versus T , with the same color code. $J^m = 1, J_{mf1} = -0.15, J_{mf2} = 0.8$ corresponding to the GS with energy E_2 .

parameters. We can see that in this case the magnetic subsystem does not undergo a phase transition as a ferromagnet in a field. On the contrary, there is a second-order transition for ferroelectric layers at $T_c \simeq 1.84$.

With increasing J_{mf} , the system undergoes a first-order transitions. Fig. 8 shows the total magnetization M and susceptibility versus T for several values of J_{mf} in the cross-over region from second to first order. The second-order phase transitions starts at $J_{mf} = 0$ with $T_c \approx 2.456$, it decreases as J_{mf} increases.

We show in Fig. 9 the case of $J_{mf} = -9.5$ where one can observe a discontinuity at the transition temperature $T_c \simeq 3.45$ for the interface magnetic layer and $T_c \simeq 3.49$ for the interface ferroelectric layer. Only layer 1 and 4 for magnetic and ferroelectric systems have a phase transition. Their order parameters strongly fall down at the transition temperature.

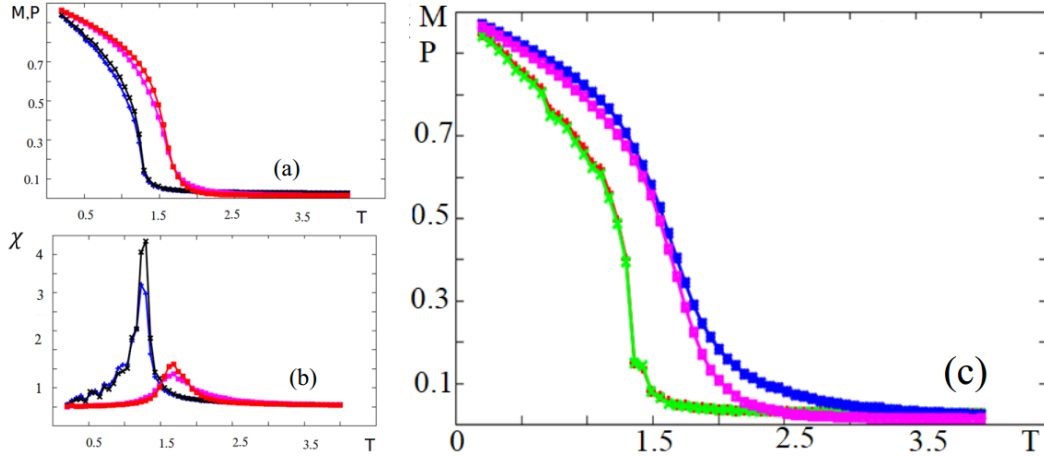


FIG. 6: (a) Temperature dependence of layer magnetizations and layer polarizations, (b) layer susceptibilities, in the case $J^m = 1$, $J^f = 1$, $J_{mf} = -0.15$, $H^z = E^z = 0$, $L = 40$, $L_z = 8$. Blue squares for the first layer and fourth magnetic layers (interface layers), black circles for the second and third (interior magnetic layers), magenta squares for the first and fourth (interface) ferroelectric layers, red for the second and third interior ferroelectric layers, respectively. $J_{mf1} = J_{mf2}$; (c) Temperature dependence of layer magnetizations and polarizations for $J^m = 1$, $J^f = 1$, $J_{mf} = -0.55$, $H^z = E^z = 0$, $|\vec{S}| = 1$, $P = \pm 1$. The coupling used is Eq. (24). Red and green lines are for magnetic interface and inner layers, magenta (blue) line for the interface (inner) ferroelectric layer.

This result is confirmed by several independent simulations. We calculate the transition temperature as a function of J_{mf} . We keep J_{mf} constant, change the temperature and we take the transition temperature at the peak of the magnetic and ferroelectric susceptibility χ . Note that for the strong interface coupling $J_{mf} = -9.5$, the interface order (black and blue curves in Fig. 9b) is so strong that it acts on the interior layer as an external field which does not allow the interior layer order parameter to go to zero: as a consequence, the interior layer undergoes only a smooth change of curvature at $T \simeq 1.5$ and falls to zero with the interface magnetic layer at $T_c \simeq 3.45$ (see red curve in Fig. 9b).

The results for the transition temperature T_c are shown in Fig. 10 as a function of J_{mf} . One can see that the transition temperature increases when we increase the values of $|J_{mf}|$.

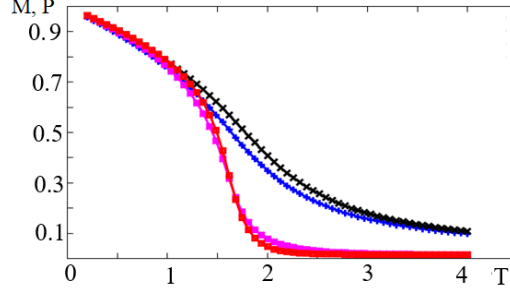


FIG. 7: Temperature dependence of layer magnetizations and layer polarizations in case $J^m = 1$, $J^f = 1$, $J_{mf}(= J_{mf1} = J_{mf2}) = -0.15$, $H^z = 0.7$ and $E^z = 0$, $L = 40$, $L_z = 8$. Blue squares for the first layer and fourth magnetic layers (interface layers), black circles for the second and third (interior magnetic layers), magenta squares for the first and fourth (interface) ferroelectric layers, red for the second and third interior ferroelectric layers, respectively.

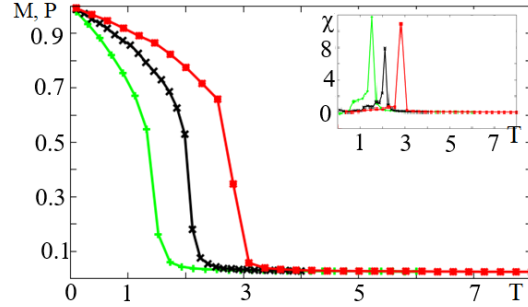


FIG. 8: Temperature dependence of the total magnetization and susceptibility in case $J^m = 1$, $J^f = 1$, $J_{mf} = -1, -3, -5.5$, $H^z = E^z = 0$, $L = 40$, $L_z = 8$. Red lines for $J_{mf} = -5.5$, black lines for $J_{mf} = -3$, green lines for $J_{mf} = -1$.

T_c has a maximum at $J_{mf} = -8.5$. The second-order phase transition starts at $J_{mf} = 0$ and becomes a first-order phase transition below $J_{mf} = -9$ (see Fig. 9 for $J_{mf} = -9.5$).

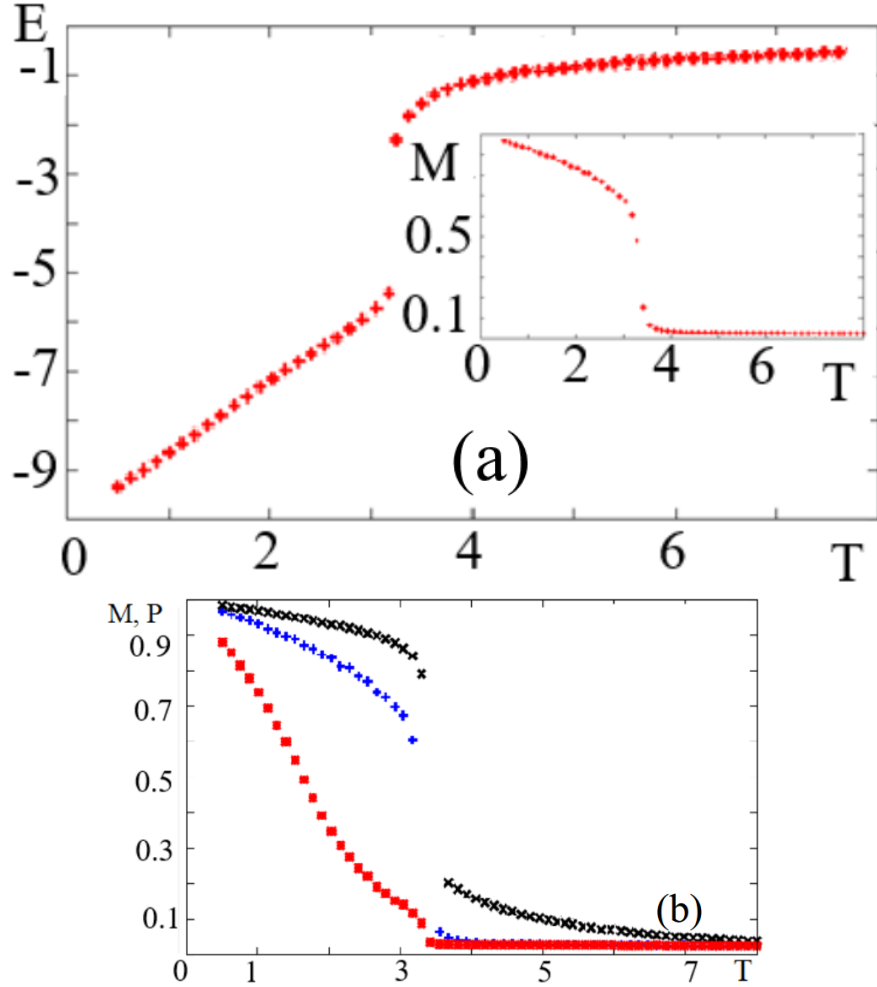


FIG. 9: (a) Energy, layer magnetization (inset) versus T ; (b) Interface layer magnetization (blue +), interior layer magnetization (red squares), interface polarization (black X) and interior layer polarization (magenta X overlapped under red squares), versus T . $J^m = 1$, $J^f = 1$, $J_{mf} = -9.5$, $H^z = E^z = 0$ $L = 40$, $L_z = 8$.

IV. ANOTHER MODEL OF INTERFACE INTERACTION

Let us show some results for the another model of magnetoelectric interaction given in the form

$$H_{mf}^1 = -J_{mf} \sum_{i,j,k} P_i P_j S_i^z \quad (22)$$

We show in Fig. 12 layer magnetizations and polarizations as functions of interface coupling J_{mf} . For small values of the magnetoelectric interaction, magnetic and ferroelectric layers undergo phase transitions of different orders: magnetic layers undergo a phase tran-

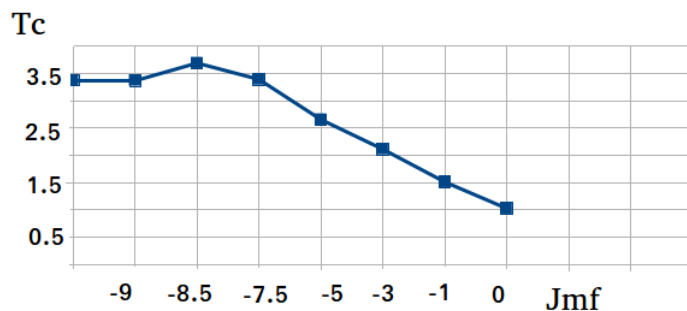


FIG. 10: Phase diagram in $T - J_{mf}$ plane. Here $J^m = 1$, $J^f = 1$, $H^z = E^z = 0$.

sition of the first order, while ferroelectric layers undergo a the second-order transition, at temperatures $T_c \approx 0.63$ and $T_c \approx 1.52$, respectively.

With an increase of the magnetoelectric interaction J_{mf} between the magnetic and ferroelectric subsystems, an unusual phenomenon is observed: the interface layers after $J_{mf} = -3.5$ undergo phase transitions of the first order. Note that in the model considered at the beginning of this article this occurs at large values of $J_{mf} = -9.5$. This is shown in Fig. 12a for the magnetic subsystem and in the inset for the ferroelectric layers.

For the inner layers of the magnetic subsystem, as the parameter J_{mf} increases, the type of transition changes (Fig. 12b).

Phase diagram in Fig. 13a shows the effect of J_{mf} on the transition temperature of the interface magnetic and ferroelectric layers. One can see that the transition temperature increases as the absolute value of J_{mf} increases. At $J_{mf} = -3$ and below the transition temperatures for the magnetic and ferroelectric layers become distinct.

Phase diagram in Fig. 13b shows the effect of the external electric field E on the transition temperature of the interface magnetic and ferroelectric layers. One finds that the transition temperature is almost unchanged when we increase E^z up to $E^z = 0.5$. For large values of $|J_{mf}|$ ($J_{mf} \ll -3$) the transition temperature is not sensitive to E^z .

Figure 11 shows the effect of the competition between the magnetoelectric interaction and the external electric field. With moderate magnetoelectric interaction ($J_{mf} = -2.5$), we can remark that the interface ferroelectric layer undergoes a second-order phase transition at $T_c = 1.77$, the magnetic layers undergo a second-order phase transition at $T_c = 1.64$. When we include an external electric field, both subsystems undergo a first-order phase transition

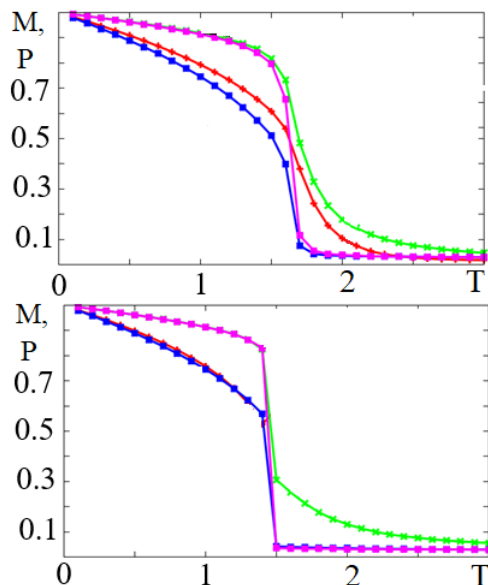


FIG. 11: Temperature dependence of layer magnetizations and polarizations for $J^m = 1$, $J^f = 1$, $J_{mf} = -2.5$, $H^z = 0$, with $E^z = 0$ (top) and $E^z = 0.5$ (bottom). The coupling is given by H_{mf}^1 (Eq. 22). Color code: magenta (or purple) lines for the first layer and fourth magnetic layers (interface layers), blue lines for the second and third (interior magnetic) layers. Green lines for the first and fourth (interface) ferroelectric layers, red lines for the second and third interior ferroelectric layers, respectively.

at the same temperature $T_c = 1.5$.

If the magnetoelectric interaction has a large value and the external electric field is zero, we have seen above that the interface magnetic and ferroelectric layers undergo a first-order phase transition. The inner magnetic layer undergoes a second-order phase transition while the internal ferroelectric layers are not subject to a phase transition. Now if we apply an electric field for instance $E^z = 0.5$, the inner ferroelectric layers undergo a second-order phase transition (not shown).

To conclude this section, let us emphasize that beyond the two models for interface coupling studied above, the Dzyaloshinskii-Moriya interface interaction of the form $J_{mf} \vec{P}_k \cdot (\vec{S}_i \times \vec{S}_j)$ may induce unexpected phenomena at the magneto-ferroelectric interface^{28,29}. Work is under way to investigate this coupling model.

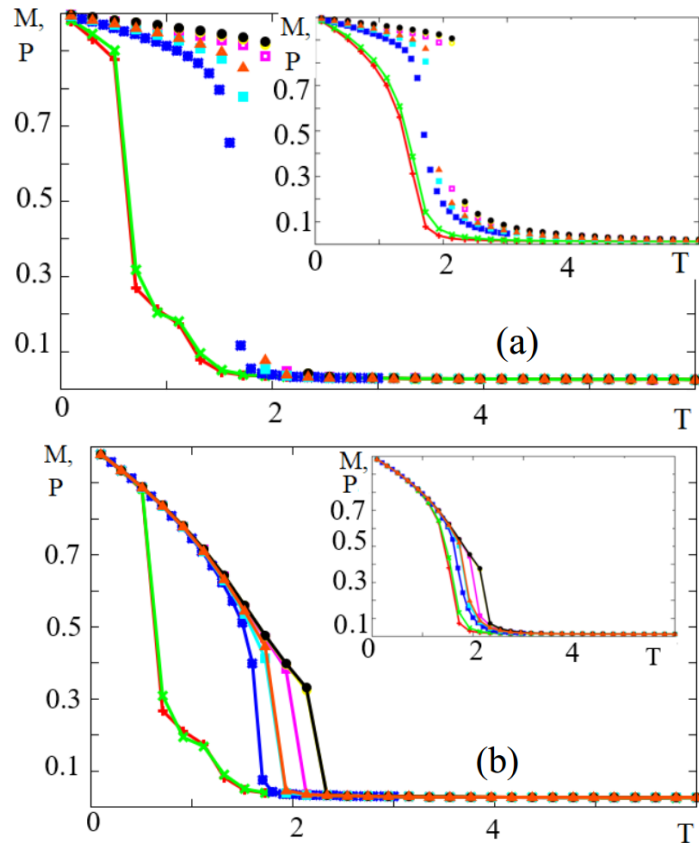


FIG. 12: (a) Temperature dependence of interface layers of magnetic and ferroelectric films (inset) for $J^m = 1$, $J^f = 1$, $H^z = E^z = 0$. Red line for the case $J_{mf} = -0.25$, green line for $J_{mf} = -0.5$. Blue points: $J_{mf} = -2.5$, light blue points: $J_{mf} = -3.5$, black points: $J_{mf} = -7$; (b) Temperature dependence of interior layers of magnetic and ferroelectric films (inset) with the same parameters and color code. The coupling is given by H_{mf}^1 .

V. MEAN-FIELD THEORY

Let us show some analytical results obtained by us using the mean-field (MF) theory for the Hamiltonian

$$\mathcal{H} = H_m + H_f + H_{mf}, \quad (23)$$

where

$$H_{mf} = -J_{mf} \sum_{i,j,k} \vec{S}_i \cdot \vec{S}_j P_k, \quad (24)$$

We consider the spin at the site i and ferroelectric polarization at the site l . We can write their local fields from the NN as

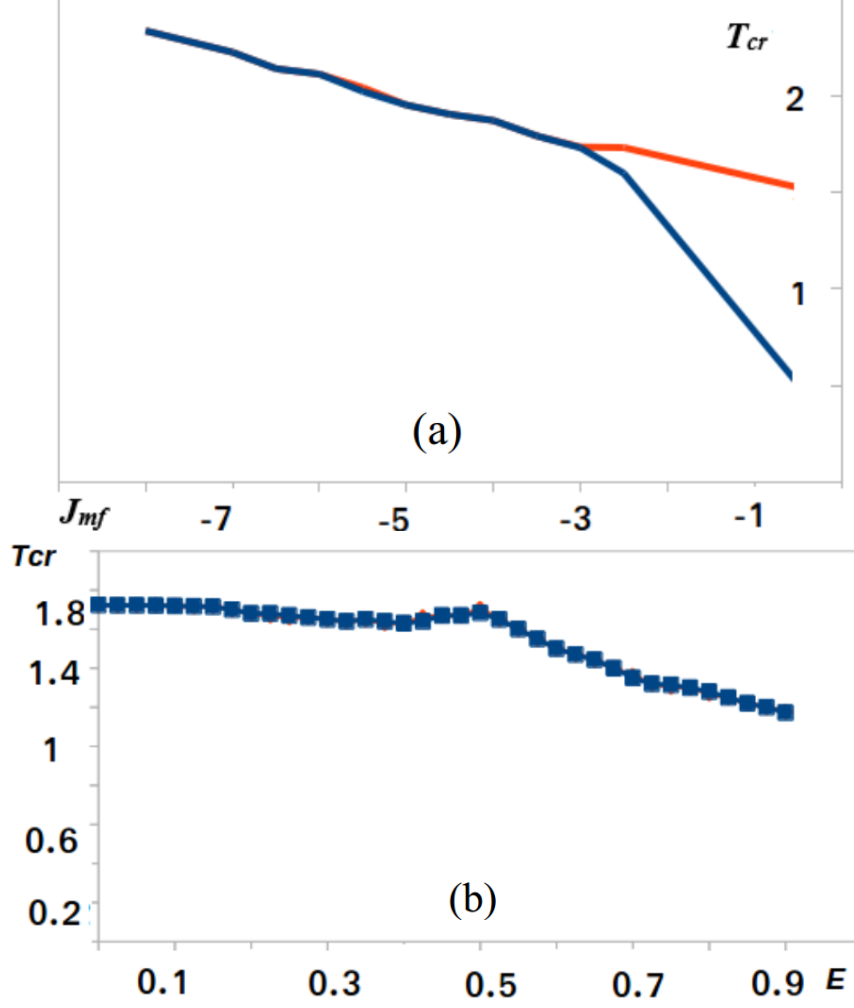


FIG. 13: (a) Phase diagram in $T - J_{mf}$ plane. Here $J^m = 1$, $J^f = 1$, $H^z = E^z = 0$. Red line and black line are for the ferroelectric critical temperature and the magnetic critical temperature, respectively. The coupling is given by H_{mf}^1 ; (b) Phase diagram in $T - E$ plane (E stands for E^z). Here $J^m = 1$, $J^f = 1$, $H^z = 0$, $J_{mf} = -3.5$.

$$H_i = -J^m \sum_{\vec{p}} \vec{S}_i \cdot \vec{S}_{i+p} - \vec{H} \cdot \vec{S}_i - \frac{J_{mf}}{2} \delta_{i,4} P_{i+1} \sum_{\vec{p}} \vec{S}_i \cdot \vec{S}_{i+p} \quad (25)$$

$$H_l = -J^f \sum_{\vec{p}} P_l P_{l+p} - E^z P_l - \frac{J_{mf}}{2} \delta_{l,5} \sum_{\vec{p}} P_l \vec{S}_{l-1} \cdot \vec{S}_{l+1+p} \quad (26)$$

or

$$H_i = -\vec{H} S_i^z \quad (27)$$

$$H_l = -\vec{H}_2 P_l \quad (28)$$

here

$$\bar{H} = \xi_i(\langle S_z \rangle + \langle \Delta S_z \rangle) + H^z \quad (29)$$

$$\bar{H}_2 = J_f C_3(\langle P_z \rangle + \langle \Delta P_z \rangle) - \frac{J_{mf}}{2} \delta_{l,5} C_2 S_{l-1}^z (\langle S_z \rangle + \langle \Delta S_z \rangle) + E^z \quad (30)$$

$$\xi_i = J_m C_1 - \frac{J_{mf}}{2} \delta_{i,4} C_2 P_{i+1} \quad (31)$$

where for notation convenience we write P_z instead of P .

We choose the z axis for the spin quantization axis. The average value of the xy spin components are then zero since the spin precesses circularly around the z axis:

$$\langle S_{i+p}^x \rangle = \langle S_{i+p}^y \rangle = \langle S_{l-1+p}^x \rangle = \langle S_{l-1+p}^y \rangle = 0 \quad (32)$$

$$\langle S^z \rangle + \langle \Delta S^z \rangle = \frac{\sum_{S_i^z=-S}^S S_i^z \exp(-\beta H_i)}{Z_i} \quad (33)$$

where the partition function is

$$Z_i = \sum_{S_i^z=-S}^S \exp(-\beta H_i) = \sum_{S_i^z=-S}^S S_i^z \exp(-\beta \bar{H} S_i^z) \quad (34)$$

$$Z_i = \frac{\sinh(\beta \bar{H} (S + \frac{1}{2}))}{\sinh(\frac{1}{2} \beta \bar{H})} \quad (35)$$

where

$$S = |\vec{S}_i| \quad (36)$$

We obtain

$$\langle S^z \rangle + \langle \Delta S^z \rangle = B_S(\beta S \bar{H}) \quad (37)$$

here $B_S(\beta S \bar{H})$ is the Brillouin function defined by

$$B_S(\beta S \bar{H}) = \frac{2S+1}{2S} \coth\left(\frac{(2S+1)\beta S \bar{H}}{2S}\right) - \frac{1}{2S} \coth\left(\frac{\beta S \bar{H}}{2S}\right) \quad (38)$$

If H^z is very weak, we can suppose that $\langle \Delta S^z \rangle \rightarrow 0$ and in such a case we can expand the Brillouin function near $x_0 = \beta \xi_i S \langle S^z \rangle$

$$\langle \Delta S^z \rangle = \frac{S}{k_B T} (S H^z + S \xi_i \langle \Delta S^z \rangle) \frac{\partial B_S(x_0)}{\partial x_0} \quad (39)$$

If $H^z = 0$ then

$$\langle S^z \rangle = S B_S(x_0) \quad (40)$$

At high temperature $\beta\langle S^z \rangle \ll 1$ and

$$B_S(\beta S \bar{H}) \approx \frac{S+1}{3S} \beta S \bar{H} - \frac{[S^2 + (S+1)^2](S+1)}{90S^3} (\beta S \bar{H})^3 + O((\beta S \bar{H})^5) \quad (41)$$

The previous equation becomes

$$\langle S^z \rangle \left[\frac{\xi_i S(S+1)}{3k_B T} - 1 \right] = \frac{S(S+1)[S^2 + (S+1)^2]}{90} \left(\frac{\xi_i}{k_B T} \right)^3 (\langle S^z \rangle)^3 \quad (42)$$

This equation has a solution $\langle S^z \rangle \neq 0$ only if

$$\frac{(2J_m C_1 + J_{mf} \delta_{i,4} P_{i+1} C_2) S(S+1)}{6k_B T} - 1 > 0 \quad (43)$$

namely

$$T < \frac{2J_m C_1 + J_{mf} \delta_{i,4} P_{i+1} C_2 S(S+1)}{6k_B} = T_c \quad (44)$$

for H_l we can write in the same manner the MF equations, and one can obtain for $\langle P^z \rangle + \langle \Delta P^z \rangle$

$$\langle P^z \rangle + \langle \Delta P^z \rangle = P B_P(\beta P \bar{H}_2) \quad (45)$$

where $B_P(\beta P \bar{H}_2)$ is the Brillouin function defined by

$$B_P(\beta P \bar{H}_2) = \frac{2P+1}{2P} \coth\left(\frac{(2P+1)\beta P \bar{H}_2}{2P}\right) - \frac{1}{2P} \coth\left(\frac{\beta P \bar{H}_2}{2P}\right) \quad (46)$$

In zero applied electric field we can write

$$\langle P^z \rangle = P B_P(y_0) \quad (47)$$

here

$$y_0 = \frac{1}{k_B T} (J_f C_1 P \langle P^z \rangle + y_1 (\langle S^z \rangle) + \langle \Delta S^z \rangle) \quad (48)$$

$$y_1 = J_{mf} \frac{P}{2} C_2 \delta_{l,5} S_{l-1}^z \quad (49)$$

At high temperature, $\langle P^z \rangle = P B_P(y_0)$ becomes

$$\begin{aligned} \langle P^z \rangle &= \frac{P+1}{k_B T} (J_f C_3 P \langle P^z \rangle) + y_1 (\langle S^z \rangle - \langle \Delta S^z \rangle) \\ &\quad - \frac{(P^2 + (P+1)^2)(P+1)}{90P^3} \left(\frac{J_f C_3 P \langle P^z \rangle}{k_B T} + y_1 (\langle S^z \rangle - \langle \Delta S^z \rangle)^3 \right) \end{aligned} \quad (50)$$

For our superlattice we can obtain for each layer the following system of equations

$$\langle S_{1,4}^z \rangle + \langle \Delta S_{1,4}^z \rangle = S B_{\varphi_{1-4}} + S U_{\psi_{1-4}} \quad (51)$$

$$B_{\varphi_{1-4}} = B_S \left(\left(\frac{J_m SC_1}{k_B T} + \frac{J_{mf} SC_2}{k_B T} \langle P_{5,8}^z \rangle \right) \langle S_{1,4}^z \rangle + \frac{J_m S}{k_B T} \langle S_{2,3}^z \rangle \right) \quad (52)$$

$$U_{\psi_{1-4}} = \left(\frac{J_m SC_1}{k_B T} + \frac{J_{mf} SC_2}{k_B T} \langle P_{5,8}^z \rangle \right) \langle \Delta S_{1,4}^z \rangle + \frac{H S^2}{k_B T} \frac{\partial B_S(u)}{\partial u} \quad (53)$$

$$u = \left(\frac{J_m SC_1}{k_B T} + \frac{J_{mf} SC_2}{k_B T} \langle P_{5,8}^z \rangle \right) \langle S_{1,4}^z \rangle \quad (54)$$

$$\langle S_2^z \rangle + \langle \Delta S_2^z \rangle = S B_{\varphi_2} + S U_{\psi_2} \quad (55)$$

$$B_{\varphi_2} = B_S \left(\frac{J_m SC_1 \langle S_2^z \rangle}{k_B T} + \frac{J_{mf} S \langle S_{1,4}^z \rangle \langle P_{7,8}^z \rangle}{k_B T} + \frac{J_m S \langle S_3^z \rangle}{k_B T} \right) \quad (56)$$

$$U_{\psi_2} = -S^2 \left(\frac{J_m C_1 \langle \Delta S_2^z \rangle}{k_B T} + \frac{H}{k_B T} \right) \frac{\partial B_S \left(\frac{J_m SC_1 \langle S_{1,4}^z \rangle}{k_B T} \right)}{\partial \left(\frac{J_m SC_1 \langle S_{1,4}^z \rangle}{k_B T} \right)} \quad (57)$$

$$\langle S_3^z \rangle + \langle \Delta S_3^z \rangle = S B_{\varphi_3} + S U_{\psi_3} \quad (58)$$

$$B_{\varphi_3} = B_S \left(\frac{J_m SC_1 \langle S_3^z \rangle}{k_B T} + \frac{J_{mf} S \langle S_2^z \rangle \langle P_{7,8}^z \rangle}{k_B T} + \frac{J_m S \langle S_{1-4}^z \rangle}{k_B T} \right) \quad (59)$$

$$U_{\psi_3} = -S^2 \left(\frac{J_m C_1 \langle \Delta S_3^z \rangle}{k_B T} + \frac{H}{k_B T} \right) \frac{\partial B_S \left(\frac{J_m SC_1 \langle S_{1,4}^z \rangle}{k_B T} \right)}{\partial \left(\frac{J_m SC_1 \langle S_{1,4}^z \rangle}{k_B T} \right)} \quad (60)$$

$$\langle P_{5,8}^z \rangle + \langle \Delta P_{5,8}^z \rangle = P B_{\varphi_{5,8}} + P U_{\psi_{5,8}} \quad (61)$$

$$B_{\varphi_{5,8}} = B_P \left(\frac{J_f PC_3 \langle P_{5,8}^z \rangle}{k_B T} + \frac{J_{mf} PC_2 (\langle S_{1,4}^z \rangle)^2}{k_B T} + \frac{J_f P \langle P_6^z \rangle}{k_B T} \right) \quad (62)$$

$$U_{\psi_{5,8}} = -P^2 \left(\frac{J_f C_3 \langle \Delta P_{5,8}^z \rangle}{k_B T} + \frac{J_{mf} C_2 (\langle S_{1,4}^z \rangle)^2}{k_B T} + \frac{E}{k_B T} \right) \frac{\partial B_P(v)}{\partial v} \quad (63)$$

$$v = \frac{J_f PC_3 \langle P_{5,8}^z \rangle}{k_B T} + \frac{J_{mf} PC_2 (\langle S_{1,4}^z \rangle)^2}{k_B T} \quad (64)$$

$$\langle P_6^z \rangle + \langle \Delta P_6^z \rangle = P B_{\varphi_6} + P U_{\psi_6} \quad (65)$$

$$B_{\varphi_6} = B_P \left(P \left(\frac{J_f C_3 \langle P_6^z \rangle}{k_B T} + \frac{J_{mf} P (\langle S_{1,4}^z \rangle)^2}{k_B T} + \frac{J_f \langle P_7^z \rangle}{k_B T} \right) \right) \quad (66)$$

$$U_{\psi_6} = -P^2 \left(\frac{J_f C_3 \langle \Delta P_6^z \rangle}{k_B T} + \frac{E}{k_B T} \right) \frac{\partial B_P \left(\frac{J_f PC_3}{k_B T} \right)}{\partial \left(\frac{J_f PC_3}{k_B T} \right)} \quad (67)$$

$$\langle P_7^z \rangle + \langle \Delta P_7^z \rangle = P B_{\varphi_7} + P U_{\psi_7} \quad (68)$$

$$B_{\varphi 7} = B_P \left(\frac{J_f P C_3 \langle P_7^z \rangle}{k_B T} + \frac{J_{mf} P (\langle S_{1,4}^z \rangle)^2}{k_B T} + \frac{J_f P \langle P_6^z \rangle}{k_B T} \right) \quad (69)$$

$$U_{\psi 7} = -P^2 \left(\frac{J_f C_3 \langle \Delta P_7^z \rangle}{k_B T} + \frac{E}{k_B T} \right) \frac{\partial B_P \left(\frac{J_f P C_3}{k_B T} \right)}{\partial \left(\frac{J_f P C_3}{k_B T} \right)} \quad (70)$$

Figure 14 shows the effect of the magnetoelectric interaction on the temperature dependence of the polarization and the magnetization, for both the interface and the inner layer. In the MF theory, the magnetization and ferroelectric polarization coincide if their amplitudes are the same. This is because the xy spin components are neglected, making Heisenberg spins S equivalent to Ising spins P .

If we compare Figs. 14 and 4-6 one can see an agreement between MC and MF theory that the interface order parameter depends strongly on the interface coupling and have different value from that of the interior layers.

If we take $|P| = 1.5$ we see different transition temperatures for magnetic and ferroelectric films as seen in Figure 15.

VI. CONCLUSION

We have studied in this paper the effects of the temperature, external magnetic and electric fields, the magnetoelectric coupling in a multiferroic superlattice formed by alternating magnetic and ferroelectric films. Magnetic films in this work were modeled as films of simple cubic lattice with Heisenberg spins. Electrical polarizations of values ± 1 were assigned at each lattice site in the ferroelectric films.

We have studied these superlattices with MC simulations and with a MF theory. Various physical quantities have been obtained to identify and characterize the phase transition in each subsystem as functions of temperature T , interface coupling parameter and applied magnetic and electric fields. Two models of interface coupling have been considered. The MC and MF calculations agree with each other with regard to the interface order parameters.

Among our MC results let us mention the change of the nature of the phase transition when the interface coupling parameter changes. Various phase diagrams have been established which show that magnetic and ferroelectric phase transitions are closely connected. The interface magnetic and ferroelectric layers have distinct behaviors compared to the inner

layers. This is known when there is a loss of translation invariance such as the presence of an impurity, a surface or an interface.

We have worked out a laborious mean-field formalism for superlattices. The application of this in this paper was intentionally limited, but there are wider applications in many system geometries and in various interacting films such as ferri-electric superlattices and frustrated superlattices which have not been considered here.

To conclude, let us emphasize that we have studied in this work two models for interface coupling. Other models of interface magneto-ferroelectric coupling such as the Dzyaloshinskii-Moriya interaction may induce unexpected phenomena at the magneto-ferroelectric interface. Work is under way to investigate this coupling model.

Acknowledgment

One of us (IFS) wishes to thank Campus France for a financial support (contract P678172A) during the course of the present work.

References

-
- ¹ H. T. Diep, *Theory Of Magnetism - Application to Surface Physics*, World Scientific, 2014.
 - ² H. T. Diep, Theoretical methods for understanding advanced magnetic materials: The case of frustrated thin films, *Journal of Science: Advanced Materials and Devices* 1 (1) (2016) 31 – 44.
 - ³ V. V. Prudnikov, P. V. Prudnikov, D. E. Romanovskii, Monte carlo simulation of multilayer magnetic structures and calculation of the magnetoresistance coefficient, *JETP Letters* 102 (10) (2015) 668–673.
 - ⁴ M. K. Ramazanov, A. K. Murtazaev, Phase transitions in the antiferromagnetic layered ising model on a cubic lattice, *JETP Letters* 103 (7) (2016) 460–464.
 - ⁵ I. K. Kamilov, A. K. Murtazaev, K. K. Aliev, Monte carlo studies of phase transitions and critical phenomena, *Physics-Uspekhi* 42 (7) (1999) 689–709.
 - ⁶ A. P. Pyatakov, A. K. Zvezdin, Magnetolectric and multiferroic media, *Physics-Uspekhi* 55 (6) (2012) 557–581.

- ⁷ Y. Weng, L. Lin, E. Dagotto, S. Dong, Inversion of ferrimagnetic magnetization by ferroelectric switching via a novel magnetoelectric coupling, *Phys. Rev. Lett.* 117 (2016) 037601.
- ⁸ K. Iijima, T. Terashima, Y. Bando, K. Kamigaki, H. Terauchi, Atomic layer growth of oxide thin films with perovskitetype structure by reactive evaporation, *Journal of Applied Physics* 72 (7).
- ⁹ D. O'Neill, R. M. Bowman, J. M. Gregg, Dielectric enhancement and maxwellwagner effects in ferroelectric superlattice structures, *Applied Physics Letters* 77 (10).
- ¹⁰ B. D. Qu, W. L. Zhong, R. H. Prince, Interfacial coupling in ferroelectric superlattices, *Phys. Rev. B* 55 (1997) 11218–11224.
- ¹¹ R. Ramesh, N. A. Spaldin, Multiferroics: progress and prospects in thin films, *Nature materials* 6 (1) (2007) 21–29.
- ¹² Y. Magnin, H. T. Diep, Monte carlo study of magnetic resistivity in semiconducting mnnte, *Phys. Rev. B* 85 (2012) 184413.
- ¹³ M. K. Kharrasov, I. R. Kyzrygulov, I. F. Sharafullin, A. G. Nugumanov, Phase transitions and critical phenomena in multiferroic films with orthorhombic magnetic structure, *Bulletin of the Russian Academy of Sciences: Physics* 80 (6) (2016) 695–697.
- ¹⁴ I. A. Sergienko, E. Dagotto, Role of the dzyaloshinskii-moriya interaction in multiferroic perovskites, *Phys. Rev. B* 73 (2006) 094434.
- ¹⁵ I. V. Bychkov, D. A. Kuzmin, V. G. Shavrov, S. Lamekhov, Monte carlo modelling of two dimensional multiferroics, in: *Achievements in Magnetism*, Vol. 233 of *Solid State Phenomena*, Trans Tech Publications, 2015, pp. 379–382.
- ¹⁶ P. M. Leufke, R. Kruk, R. A. Brand, H. Hahn, *In situ* magnetometry studies of magnetoelectric lsmo/pzt heterostructures, *Phys. Rev. B* 87 (2013) 094416.
- ¹⁷ H. H. Ortiz-Alvarez, C. M. Bedoya-Hincapie, E. Restrepo-Parra, Monte carlo simulation of charge mediated magnetoelectricity in multiferroic bilayers, *Physica B: Condensed Matter* 454 (2014) 235 – 239.
- ¹⁸ V. Y. Irkhin, A new mechanism of first-order magnetization in multisublattice rare-earth compounds.
- ¹⁹ L. Gontchar, A. Nikiforov, Superexchange interaction in insulating manganites $R_{1-x}A_xMnO_3$ ($x=0, 0.5$), *Physical Review B* 66 (1) (2002) 014437.
- ²⁰ Z. Zhang, et al., Spin waves in several heisenberg systems: Three-sublattice with different

exchange constants ($j(ab) = j(bc)$ not equal $j(ca)$) and a superlattice with the elementary unit of four or three different layers.

- ²¹ H. T. Diep, H. Giacomini, Frustration - exactly solved frustrated models, in: Frustrated Spin Systems, World Scientific, 2013, pp. 1–58.
- ²² W. Wang, F.-l. Xue, M.-z. Wang, Compensation behavior and magnetic properties of a ferri-magnetic mixed-spin (1/2, 1) ising double layer superlattice, *Physica B: Condensed Matter* 515 (2017) 104–111.
- ²³ A. Feraoun, A. Zaim, M. Kerouad, Quantum monte carlo study of the electric properties of a ferroelectric superlattice, *Solid State Communications* 248 (2016) 88 – 96.
- ²⁴ D. P. Landau, K. Binder, A guide to Monte Carlo simulations in statistical physics, Cambridge university press, 2014.
- ²⁵ X. T. P. Phu, V. T. Ngo, H. T. Diep, Crossover from first-to second-order transition in frustrated ising antiferromagnetic films, *Physical Review E* 79 (6) (2009) 061106.
- ²⁶ X. T. P. Phu, V. T. Ngo, H. T. Diep, Critical behavior of magnetic thin films, *Surface Science* 603 (1) (2009) 109–116.
- ²⁷ H. T. Diep, Quantum theory of helimagnetic thin films, *Phys. Rev. B* 91 (2015) 014436.
- ²⁸ I. A. Sergienko, E. Dagotto, Role of the dzyaloshinskii-moriya interaction in multiferroic perovskites, *Physical Review B* 73 (9) (2006) 094434.
- ²⁹ H. T. Diep, S. El Hog, A. Bailly-Reyre, Skyrmion crystals: Dynamics and phase transition, *AIP Advances* 8 (5) (2018) 055707.

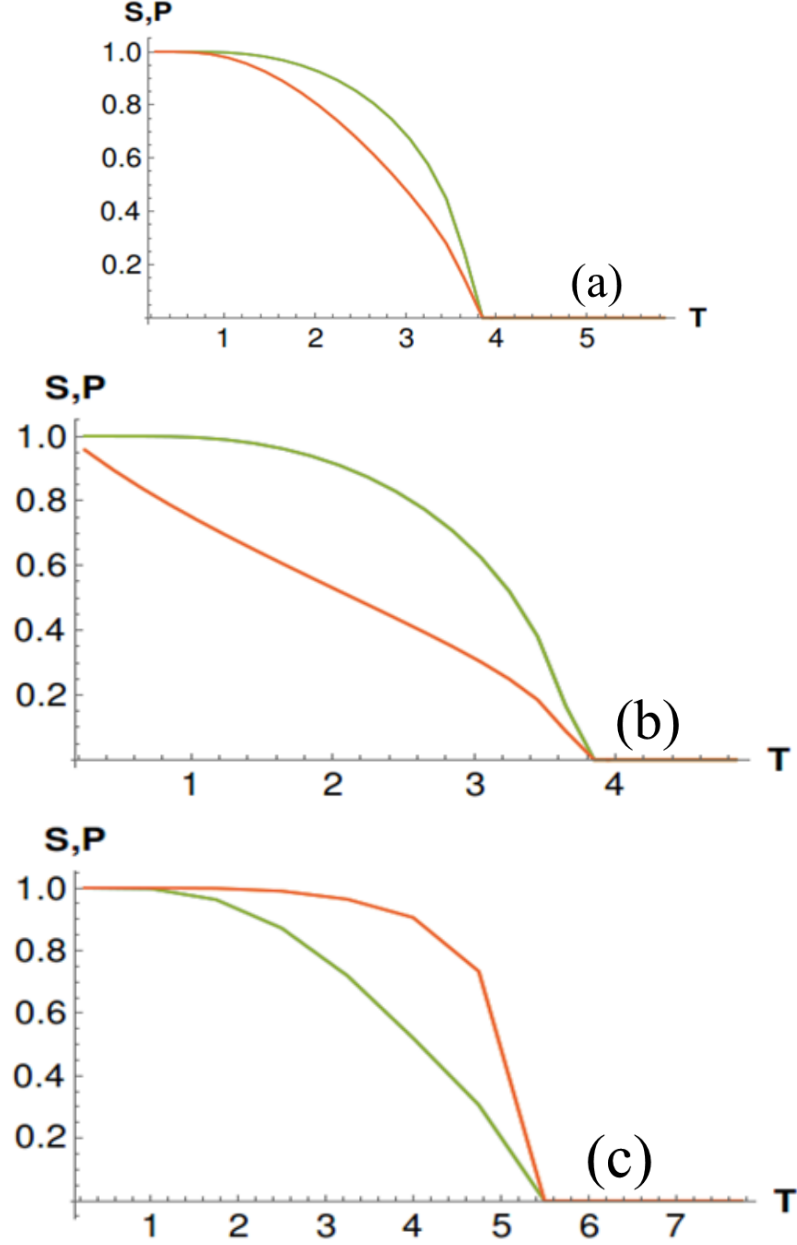


FIG. 14: Mean-field results with $J_{mf1} = J_{mf2} \equiv J_{mf}$ (a) Temperature dependence of the magnetization and polarization in the case $J^m = 1$, $J^f = 1$, $J_{mf} = -0.12$, $H^z = E^z = 0$. Red lines for the interface P and M , green line for the inner layers $M_{2,3}$ and $P_{2,3}$; (b) Temperature dependence of the magnetization and polarization in the case $J^m = 1$, $J^f = 1$, $J_{mf} = -0.55$, $H^z = 0$ and $E^z = 0$. Red lines for the interface P and M , green lines for the inner layers $M_{2,3}$ and $P_{2,3}$; (c) Temperature dependence of the magnetization and polarization in the case $J^m = 1$, $J^f = 1$, $J_{mf} = -0.85$, $H^z = E^z = 0$. Red lines for the interface P and M , green lines for the inner layers $M_{2,3}$ and $P_{2,3}$. $|\vec{S}| = |P| = 1$.

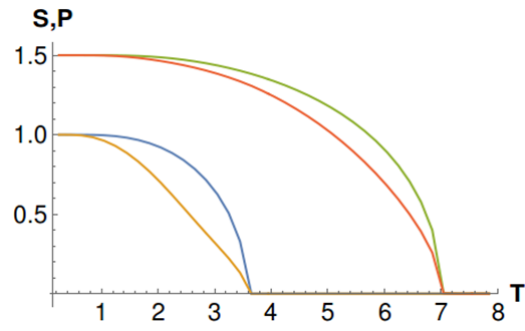


FIG. 15: Temperature dependence of the magnetization and polarization for $|\vec{S}| = 1$, $|P| = 1.5$. $J^m = -1$, $J^f = 1$, $J_{mf} = -0.12$, $H^z = E^z = 0$. Red lines for the interface P , gold line for interface M , blue line for inner layers $M_{2,3}$ and green line for inner layers $P_{2,3}$.